

# Evaluations of Hot Corrosion Behavior of Al<sub>2</sub>O<sub>3</sub> Thermal Spray Coatings with ZrO<sub>2</sub> Reinforcements on T-91 Steel

Indermeet Singh<sup>1</sup>, Khushdeep Goyal<sup>1,\*</sup>, Rakesh Goyal<sup>2</sup>

<sup>1</sup>Department of Mechanical Engineering, Punjabi University, Patiala, India  
<sup>2</sup>Chitkara Institute of Engineering and Technology, Chitkara University, Punjab, India

Copyright©2019 by authors, all rights reserved. Authors agree that this article remains permanently open access under the terms of the Creative Commons Attribution License 4.0 International License

**Abstract** Different coating with varying quantities of Al<sub>2</sub>O<sub>3</sub> and ZrO<sub>2</sub> were fabricated on the SA213 T-91 steel using plasma spray method to study hot corrosion resistance behavior. Experiment was conducted under the molten salt environment of 60% Na<sub>2</sub>SO<sub>4</sub>-40%V<sub>2</sub>O<sub>5</sub> at a temperature of 900°C inside a furnace for 50 cycles. Each cycle consisted of 1hr heating and 20 min cooling at room temperature. Results were examined using the visual inspection, weight change measurement, X-ray diffraction technique and Scanning Electron Microscopy / Energy Dispersive X-Ray Spectroscopy (SEM/EDS) analysis. Results showed that uncoated T-91 steel was more prone to hot corrosion as compared to coated steel specimens. It was noticed that ZrO<sub>2</sub> reinforcements in Al<sub>2</sub>O<sub>3</sub> coating matrix helped to enhance corrosion resistance of these coatings. The corrosion resistance increased with increase in ZrO<sub>2</sub> content in coating matrix.

**Keywords** Plasma Spray, ZrO<sub>2</sub> Coating, Al<sub>2</sub>O<sub>3</sub> Coating, Porosity, Boiler Steel

## 1. Introduction

At elevated temperature, accelerated oxidation is experienced by metal and alloys when they are exposed to corrosive environment which leads to deposition of thin film of fused salt on the surface of metal. This leads to the formation of porous non protective oxide layer on the surface and sulphides inside the substrate as described by the Gond D *et al* [1]. In boiler of a thermal power plant, corrosion occurs due to presence of sulphur in coal and oil fuels, which produce SO<sub>2</sub>, which further oxidizes partially to SO<sub>3</sub> [2, 3]. Sulphur present in fuel reacts with NaCl to form Na<sub>2</sub>SO<sub>4</sub> within the boiler tube as reported by DeCrescente and Bornstein [4]:



As the higher grade fuels are being depleted at a faster pace, therefore for production of energy, residual fuels are being used. Impurities such as Na, K, S and V are present in the residual fuel which forms low melting point compounds [5, 6]. Corrosion is initiated by these low melting compounds as they get deposited on the surface of the material. These melting compounds react with oxygen to form Na<sub>2</sub>SO<sub>4</sub> and V<sub>2</sub>O<sub>5</sub>. These compounds are known as ash. Protective oxide layer is deteriorated by these molten compounds during the boiler/gas turbine operations at high temperatures [7-9]. Different ceramics coating materials help in preventing the corrosion at elevated temperatures. Al<sub>2</sub>O<sub>3</sub> and ZrO<sub>2</sub> are preferred among the all ceramics materials because they have better chemical stability, wear resistance, superior hardness and corrosion resistance properties. Different methods of thermal coating processes are available, but plasma spray method coating is chosen because of low cost, simplicity and high deposition rate. However, fabrication of ceramic coating using plasma spray method leads to higher inherent porosity which helps the electrolyte to attack on substrate which in turn leads to corrosion. To overcome this issue bilayered coatings of Al<sub>2</sub>O<sub>3</sub> and ZrO<sub>2</sub> has been used in recent past [10, 11]. For fabrication of Al<sub>2</sub>O<sub>3</sub> coating, ZrO<sub>2</sub> is referred as underlying material for adhesion as it increases the adhesion strength as studied by Chang and Yen [12]. Even the alumina whisker is added to increase the adhesion and cohesion strength of composite coatings in the conventional coating methods. It is observed that adding ZrO<sub>2</sub> coating to aluminum alloy has sharply increased the corrosion resistance property in the salt environment. Number of cracks and black spots were also reduced and surface quality is increased by increase in weight percentage of ZrO<sub>2</sub> [13]. In the automobile industry, exhaust manifold handles high temperature and different contents of harmful gases causes the material to develop thermal stress and

corrosion [13].

It is clear from the literature study that Al<sub>2</sub>O<sub>3</sub> and ZrO<sub>2</sub> bilayered coating effectively reduced the boiler steel corrosion at higher temperature but there is a chance of inherent porosity in the substrate. There is a scope to further improve the corrosion resistance by reinforcing alumina coating matrix with ZrO<sub>2</sub> powder, instead of bilayered coatings. Therefore, it was decided to fabricate different composite coatings by reinforcing ZrO<sub>2</sub> in Al<sub>2</sub>O<sub>3</sub> coating matrix. And subsequently, their hot corrosion behavior has been studied at high temperature (900°C) in molten salt environment. So very few research have done on reinforced coating ZrO<sub>2</sub> with Al<sub>2</sub>O<sub>3</sub>.

## 2. Materials and Methods

### 2.1. Composition of Substrate Material

In this research work, SA213T-91 steel has been used as

the substrate material, because this steel alloys has been commercially used to manufacture boiler components in Indian Thermal Power Plants. The material was obtained from Guru Gobind Singh Super thermal power plant, Ropar. The chemical composition of T-91 steel alloy is given in Table 1. The sample size of substrate is 20mm×15mm×5mm were prepared by cutting the boiler steel tube.

### 2.2. Formulation of Coating

Table 2 depicts compositions and particle sizes of ZrO<sub>2</sub> and Al<sub>2</sub>O<sub>3</sub> feedstock powders used to fabricate different composite coatings.

The different coatings were fabricated at Metallizing Equipment Corporation Private Ltd. Jodhpur, Rajasthan. Plasma spray arc method was used for depositing the coatings on the substrates of T-91 boiler steel tube. All the process parameters for plasma spray method were kept at constant rate and are mentioned in Table 3.

**Table 1.** Composition of T-91 steel boiler tubes

Type of steel	ASME code	Composition	C	Mn	Si	S	Nb	P	Cr	Mo	V	Ni	Fe
T-91	SA213T-91	Actual	0.12	0.41	0.28	0.01	0.08	0.02	8.2	0.87	0.20	0.13	Bal

**Table 2.** Different coating composition on T-91 steel

Substrate Material T-91	Composition of Al <sub>2</sub> O <sub>3</sub> ( in percentage)	Composition of ZrO <sub>2</sub> ( in percentage)	Particle size
Coating 1	100	0	40±10µm
Coating 2	97	3	40±10µm
Coating 3	87	13	40±10µm
Coating 4	80	20	40±10µm

**Table 3.** Parameter used for Plasma spraying

Parameters	Values
Plasma current/A	600 A
Plasma voltage/V	50 V
Powder flow rate	50 gm/min
Arc gas (primary gas) flow rate	62 psi
Carrier gas flow	50 psi
Spray distance/mm	50

### 2.3. Experimental Set up for Hot Corrosion

The hot corrosion experiments were performed in silicon tube furnace at metallurgy lab of Chandigarh University, Mohali. The experiments were conducted at 900°C. Using the platinum- rhodium thermocouple, standardization of furnace was done and deviation of  $\pm 10^\circ\text{C}$  of temperature was shown by the indicator. Uncoated samples were mirror polished before exposing to corrosion environment and their dimension were taken using the vernier caliper so as to calculate the surface area. Samples were placed within the ceramic boats which then placed inside the furnace to carry out the hot corrosion study.

The study on coated and uncoated samples was conducted in presence of corrosive molten salt environment of Na<sub>2</sub>SO<sub>4</sub> and V<sub>2</sub>O<sub>5</sub> periodically with 50 cycles. One cycle of experiment was consisted of 1 hour of heating at 900°C followed by cooling for 20 minutes at room temperature. With number of repetitions, hot corrosion become more aggressive. Na<sub>2</sub>SO<sub>4</sub> and V<sub>2</sub>O<sub>5</sub> salts were opted, because in the lower grade fuels impurities such as sodium and vanadium are present. Mixture of Na<sub>2</sub>SO<sub>4</sub>-60%V<sub>2</sub>O<sub>5</sub> melts at lower temperature i.e. at 500°C, hence becomes highly corrosive in nature.

The study was conducted on uncoated and coated substrate and the results were compared after completion of the experiment. On all six sides of specimen mixture of Na<sub>2</sub>SO<sub>4</sub> and V<sub>2</sub>O<sub>5</sub> was applied using the camel hair brush to create a similar environment as the actual environment. The weight of each specimen after each experimental cycle was measured using the electronic weigh measuring gauge. Results were examined using the visual inspection, weight change measurement, X-ray diffraction technique and Scanning Electron Microscopy / Energy Dispersive X-Ray Spectroscopy (SEM/EDS) analysis.

## 3. Results

### 3.1. Visual Observation

The macrographs of uncoated and coated substrate of different coating compositions (100Al<sub>2</sub>O<sub>3</sub>, 97Al<sub>2</sub>O<sub>3</sub>-3ZrO<sub>2</sub>, 87 Al<sub>2</sub>O<sub>3</sub>-13 ZrO<sub>2</sub>, 80 Al<sub>2</sub>O<sub>3</sub>-20ZrO<sub>2</sub>) are shown in figure 1 after 50 cycles of exposure to hot corrosion environment. In case of T-91 uncoated substrate, blackish gray color scale started to appear after the 2<sup>nd</sup> cycle and spalling of scale was also noticed which continued up to the 50<sup>th</sup> cycle. On the other hand yellowish color started to appear on the surface of coated substrates after 5<sup>th</sup> cycle and no spallation was recorded. The variation in color indicated oxidation probability.

### 3.2. Weight Change Measurement

The hot corrosion kinetics was determined from weight change (mg/cm<sup>2</sup>) versus time plot for uncoated and coated specimens of T-91 steel. The specimens were subjected to 50 cycles of heating exposing them in molten salt environment in furnace at 900°C. The weight change data has been shown in figure 2. From the data and graph it was observed that uncoated T-91 steel experienced highest weight gain as compared to coating specimens. However it was also been noticed that with increase in percentage of ZrO<sub>2</sub>, resistance to hot corrosion increased. From figure it was clearly visible that weight gain by specimen was reduced with increase in the ZrO<sub>2</sub> in alumina matrix. The data shows that ZrO<sub>2</sub> reinforced coated specimens showed better corrosion resistance than uncoated specimen.

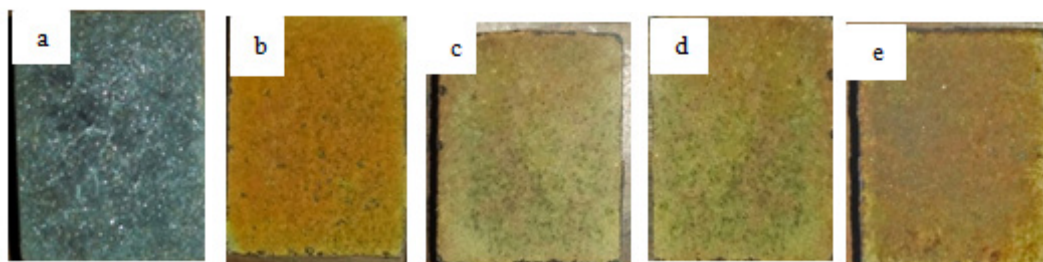


**Figure 1.** (a) T-91 uncoated (b) T-91 Al<sub>2</sub>O<sub>3</sub> (c) T-91 Al<sub>2</sub>O<sub>3</sub>-3Wt% ZrO<sub>2</sub> (d) T-91 Al<sub>2</sub>O<sub>3</sub>-13Wt% ZrO<sub>2</sub> (e) T-91 Al<sub>2</sub>O<sub>3</sub>-20Wt% ZrO<sub>2</sub>

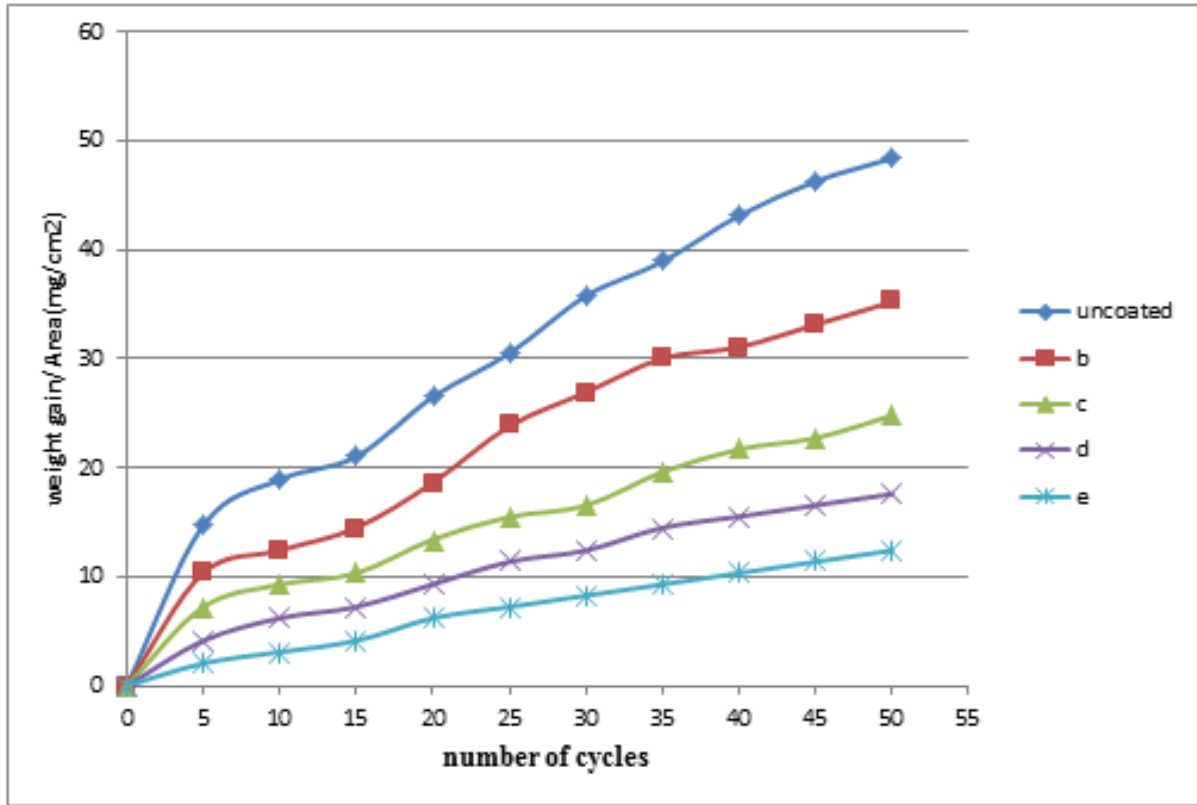


Figure 2. Weight gain plot for (a) T-91 uncoated (b) T-91 Al<sub>2</sub>O<sub>3</sub> (c) T-91 Al<sub>2</sub>O<sub>3</sub>-3Wt% ZrO<sub>2</sub> (d) T-91 Al<sub>2</sub>O<sub>3</sub>-13Wt% ZrO<sub>2</sub> (e) T-91 Al<sub>2</sub>O<sub>3</sub>-20Wt% ZrO<sub>2</sub>

### 3.3. X-ray Diffraction Analysis

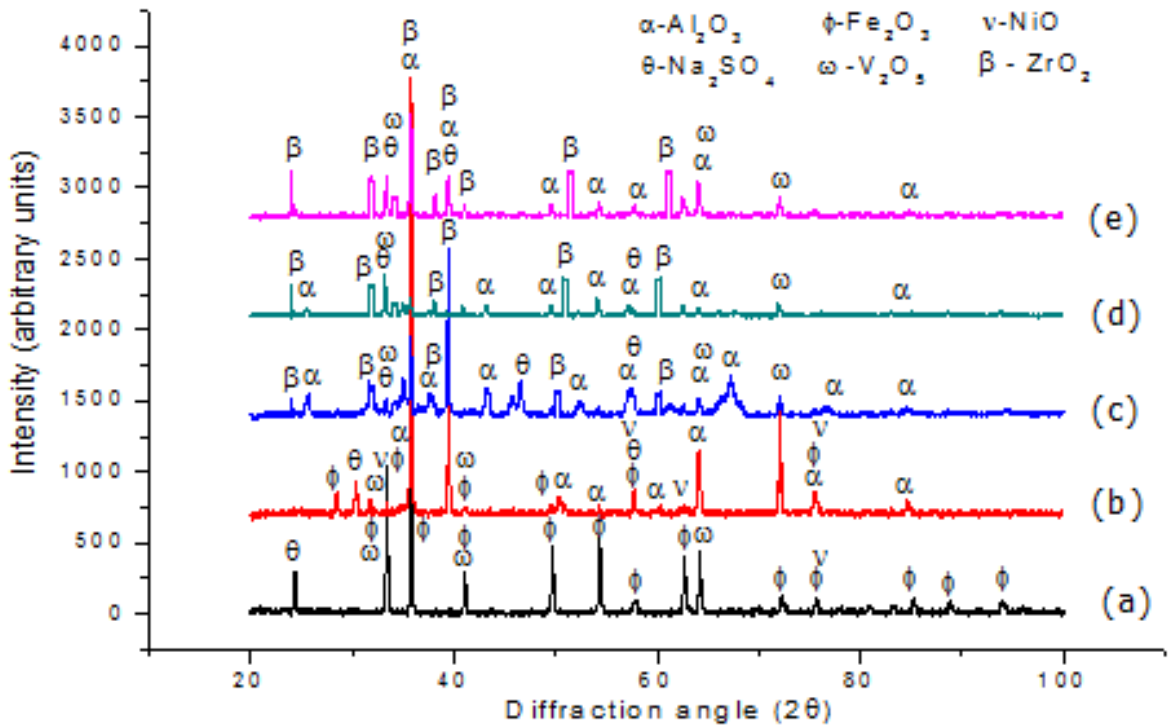


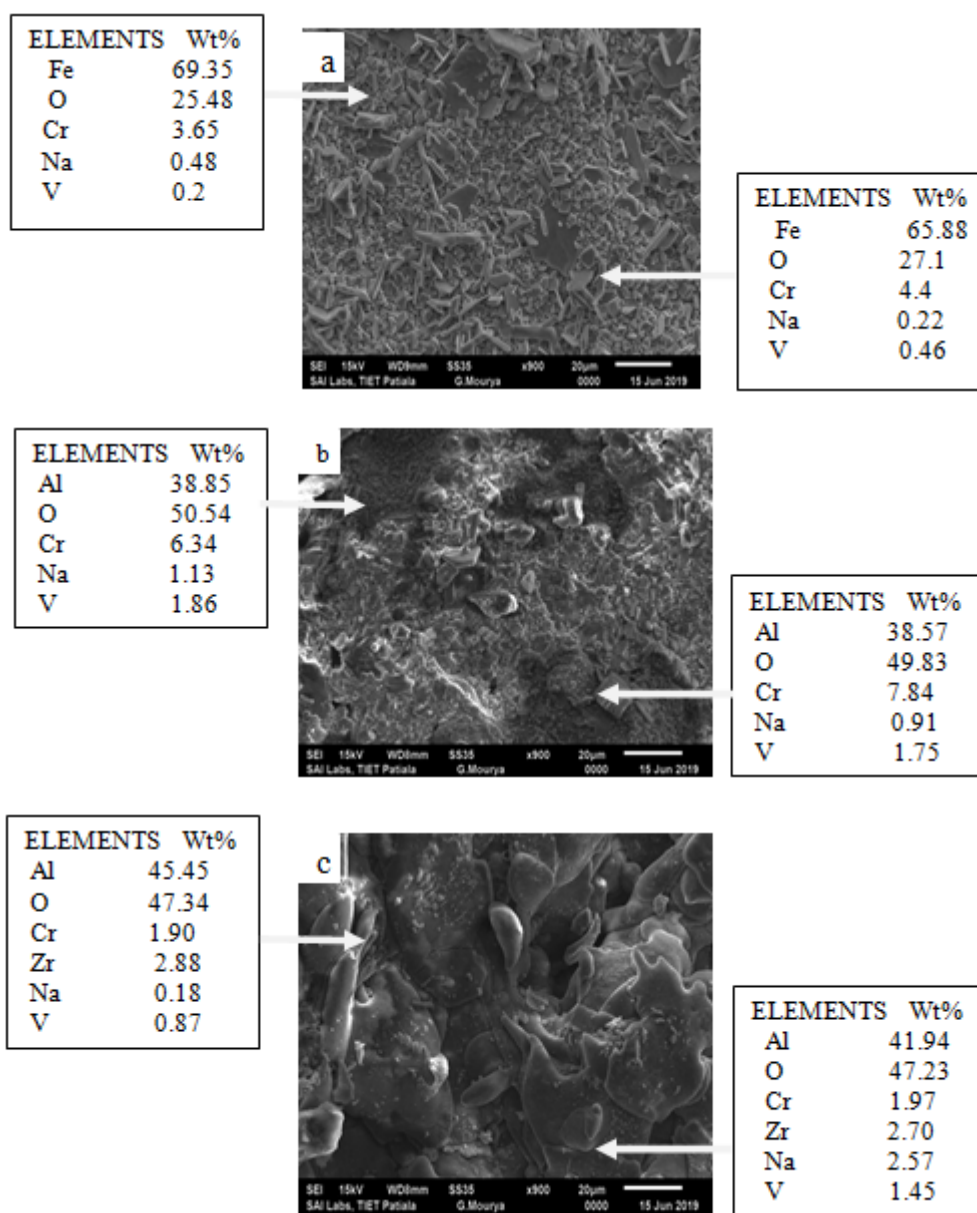
Figure 3. XRD pattern for (a) T-91 uncoated (b) T-91 Al<sub>2</sub>O<sub>3</sub> (c) T-91 Al<sub>2</sub>O<sub>3</sub>-3Wt% ZrO<sub>2</sub> (d) T-91 Al<sub>2</sub>O<sub>3</sub>-13Wt% ZrO<sub>2</sub> (e) T-91 Al<sub>2</sub>O<sub>3</sub>-20Wt% ZrO<sub>2</sub> exposed to molten salt environment for 50 cycles at a temp of 900°C

The formation of elements on the surface of corroded samples was examined using XRD analysis. Analysis indicates that the uncoated T-91 steel specimen had the presence of Fe<sub>2</sub>O<sub>3</sub> in the oxide scale (Fig. 3a). In case of Al<sub>2</sub>O<sub>3</sub> coated specimen, the peaks of Al<sub>2</sub>O<sub>3</sub> were identified along with peaks of Fe<sub>2</sub>O<sub>3</sub> (Fig. 3b). The Fe<sub>2</sub>O<sub>3</sub> might have been formed due to porosity in the alumina coating. The XRD analysis of Al<sub>2</sub>O<sub>3</sub>-3Wt% ZrO<sub>2</sub>, Al<sub>2</sub>O<sub>3</sub>-13Wt% ZrO<sub>2</sub>, Al<sub>2</sub>O<sub>3</sub>-20Wt% ZrO<sub>2</sub> coated specimens indicated presence of Al<sub>2</sub>O<sub>3</sub> and ZrO<sub>2</sub> elements in the oxide scale, with no traces of ferrous oxide (Fig. 3c-e).

EDS analysis indicated the formation of Fe<sub>2</sub>O<sub>3</sub> and Cr<sub>2</sub>O<sub>3</sub>. Micrograph shows spalling of topmost layer with badly damaged oxide scale. The scale was rich in Fe and O and small amount of Cr can be seen in the elemental analysis (Fig 4a). In case of Al<sub>2</sub>O<sub>3</sub> coated specimen (Fig. 4b), micrograph shows that it consisted of the surface morphology similar to that of plasma spray coatings. EDS analysis shows the formation of Al<sub>2</sub>O<sub>3</sub> and Cr<sub>2</sub>O<sub>3</sub>, along with presence of Fe and O. For coatings of Al<sub>2</sub>O<sub>3</sub>-3Wt% ZrO<sub>2</sub>, Al<sub>2</sub>O<sub>3</sub>-13Wt% ZrO<sub>2</sub>, Al<sub>2</sub>O<sub>3</sub>-20Wt% ZrO<sub>2</sub>, the micrographs respectively indicate no traces of corrosion and EDS analysis shows the presence of Al, Zr and O elements. ZrO<sub>2</sub> is well spotted with bright particle in darker region of Al<sub>2</sub>O<sub>3</sub> (Fig. 4c-e). Globular particles in the scale can also be observed, which might be because of the presence of excessive O, Cr.

### 3.4. SEM/EDS Analysis

Figure 4(a) shows the SEM micrograph of T-91 uncoated steel specimen after exposing it in molten salt environment for 50 cycles of heating inside a furnace. Also



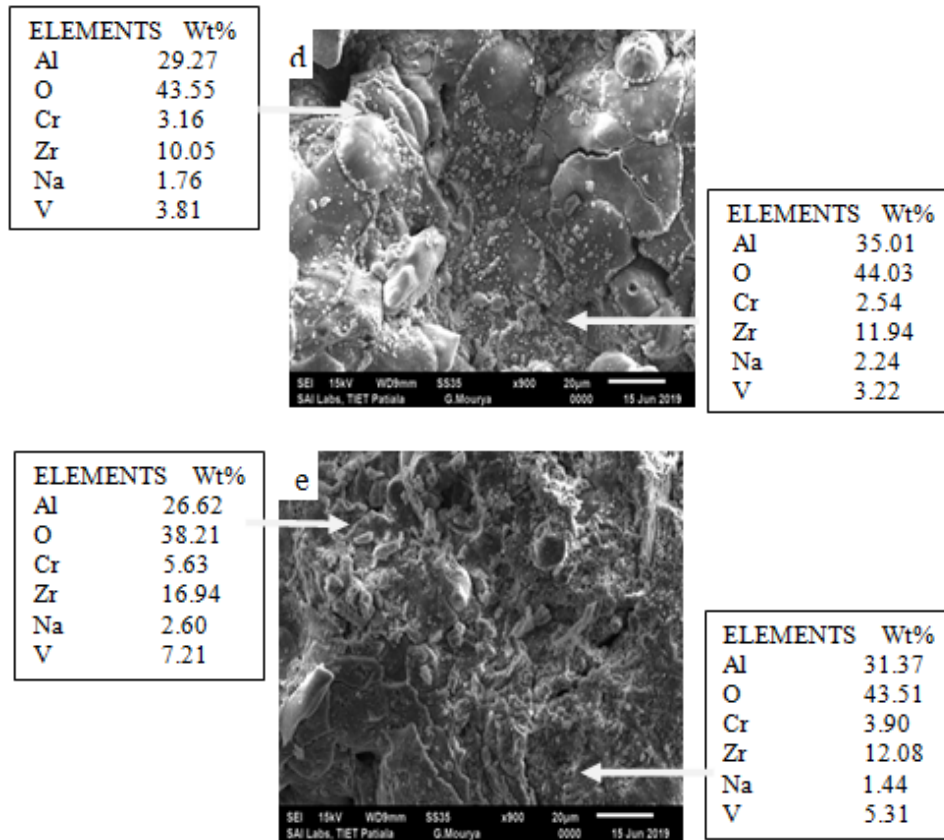


**Figure 4.** Surface scale morphology SEM images and EDS analysis for (a) T-91 uncoated (b) T-91 Al<sub>2</sub>O<sub>3</sub> (c) T-91 Al<sub>2</sub>O<sub>3</sub>-3Wt% ZrO<sub>2</sub> (d) T-91 Al<sub>2</sub>O<sub>3</sub>-13Wt% ZrO<sub>2</sub> (e) T-91 Al<sub>2</sub>O<sub>3</sub>-20Wt% ZrO<sub>2</sub>

## 4. Discussion

In this research work, different coating with varying quantities of Al<sub>2</sub>O<sub>3</sub> and ZrO<sub>2</sub> were fabricated on the SA213 T-91 steel using plasma spray method to study hot corrosion resistance behavior. Experiment was conducted under the molten salt environment of 60% Na<sub>2</sub>SO<sub>4</sub>-40%V<sub>2</sub>O<sub>5</sub> at a temperature of 900°C inside a furnace for 50 cycles. Each cycle consisted of 1hr heating and 20 min cooling at room temperature.

The uncoated T-91 boiler tube steel specimen underwent intense spalling of scale and deterioration of surface, along with color of the specimen turned to blackish grey due to severe corrosion and formation of ferrous oxide in the scale. The formation of ferrous oxide has been indicated in XRD analysis and SEM/EDS analysis. Uncoated steel experiences the internal oxidation which leads to spalling of scale, because in scale different oxides has different thermal expansion coefficient as described by Niranatlumpong et al [14]. Higher weight gain and intense spalling was due to the formation of Fe<sub>2</sub>O<sub>3</sub> which penetrated through the cracks and attacked the base metal [15]. X ray diffraction analysis indicated the formation of Fe<sub>2</sub>O<sub>3</sub> as the main constituent in uncoated steel specimen which has also been reported by Sidhu *et al* [7, 16].

The Al<sub>2</sub>O<sub>3</sub> coating on the steel alloy helped to reduce corrosion rate. The formation of Fe<sub>2</sub>O<sub>3</sub> might be due to

diffusion of Fe from the base alloy through the porosities in the alumina coating. The ZrO<sub>2</sub> reinforced Al<sub>2</sub>O<sub>3</sub> coated specimens showed no deterioration of surface and no spalling of scale was noticed. Presence of ZrO<sub>2</sub> coating increases the hardness and along with Al<sub>2</sub>O<sub>3</sub>, it increases the adhesion to the substrate steel. This helps to reduce porosities in the composite coatings. Corrosion behavior of coating and oxidation of specimens in hot corrosion is governed by mass gain. Figure 2 indicated sudden increase in mass of all specimens at initial stage. This might be due to the sudden oxygen pick-up during diffusion of oxygen at high temperature [15]. Uncoated T-91 steel specimen showed maximum increase in weight gain and Al<sub>2</sub>O<sub>3</sub>-20Wt% ZrO<sub>2</sub> showed least weight gain among all specimens. This may be due to rapid formation of oxides at grain boundaries and through small pores these oxides enters during early cycles in uncoated T-91 steel specimen as described by Niranatlumpong et al [14]. The presence of all these elements can also seen in the SEM/EDS analysis. SEM/EDS showed the higher amount of Fe<sub>2</sub>O<sub>3</sub> in uncoated steel specimen while Al<sub>2</sub>O<sub>3</sub> and ZrO<sub>2</sub> as the major element in coated specimens. ZrO<sub>2</sub> was well spotted with bright particle in darker region of Al<sub>2</sub>O<sub>3</sub>. Rate of corrosion showed the following trend: T-91 steel uncoated > Al<sub>2</sub>O<sub>3</sub> > Al<sub>2</sub>O<sub>3</sub>-3Wt% ZrO<sub>2</sub> > Al<sub>2</sub>O<sub>3</sub>-13Wt% ZrO<sub>2</sub> > Al<sub>2</sub>O<sub>3</sub>-20Wt% ZrO<sub>2</sub>.

## 5. Conclusions

The following conclusions have been drawn from this research work:

1. Using plasma spray process, different coatings of Al<sub>2</sub>O<sub>3</sub> and ZrO<sub>2</sub> have been successfully deposited on ASTM-SAE213-T-91 steel boiler.
2. XRD, SEM/EDS analysis indicated that oxide layer of uncoated T-91 steel specimen contained Fe<sub>2</sub>O<sub>3</sub> as main phase along with traces of Cr<sub>2</sub>O<sub>3</sub>.
3. Higher weight gain and intense spalling of uncoated boiler steel alloy was due to the formation of Fe<sub>2</sub>O<sub>3</sub> which penetrated through the cracks and attacked the base metal.
4. In Al<sub>2</sub>O<sub>3</sub> coating, Al<sub>2</sub>O<sub>3</sub> was noticed as major phase while Fe<sub>2</sub>O<sub>3</sub> was found as minor phase by XRD, SEM/EDS analysis. The formation of Fe<sub>2</sub>O<sub>3</sub> might be due to diffusion of Fe from the base alloy through the porosities in the alumina coating.
5. In case of Al<sub>2</sub>O<sub>3</sub>-3Wt% ZrO<sub>2</sub>, Al<sub>2</sub>O<sub>3</sub>-13Wt% ZrO<sub>2</sub>, Al<sub>2</sub>O<sub>3</sub>-20Wt% ZrO<sub>2</sub> coatings, Al<sub>2</sub>O<sub>3</sub> and ZrO<sub>2</sub> were found as major phase by XRD, SEM/EDS analysis. Small amount of globular particle was also been observed this might be because of excessive O, Cr.
6. The corrosion rate was higher for the uncoated T-91 steel as compared to the coated steel specimens.
7. The rate of corrosion was found decreasing with increase in ZrO<sub>2</sub> in alumina coating matrix and has followed following trend:  
T-91 steel uncoated > Al<sub>2</sub>O<sub>3</sub> > Al<sub>2</sub>O<sub>3</sub>-3Wt% ZrO<sub>2</sub> > Al<sub>2</sub>O<sub>3</sub>-13Wt% ZrO<sub>2</sub> > Al<sub>2</sub>O<sub>3</sub>-20Wt% ZrO<sub>2</sub>.

## REFERENCES

- [1] D. Gond, V. Chawla, D. Puri, and S. Prakash, "High Temperature Corrosion Behaviour of T-91 and T-22 Bare Steel in 75wt.% Na<sub>2</sub>SO<sub>4</sub>+ 25wt.% NaCl Molten Salt Environment at 900 C," *Journal of Minerals and Materials Characterization and Engineering*, Vol. 9, No. 07, p. 593, 2010.
- [2] K. Goyal, H. Singh, and R. Bhatia, "Behaviour of carbon nanotubes-Cr<sub>2</sub>O<sub>3</sub> thermal barrier coatings in actual boiler," *Surface Engineering*, pp. 1-11, 2019.
- [3] K. Goyal, H. Singh, and R. Bhatia, "Hot-corrosion behavior of Cr<sub>2</sub>O<sub>3</sub>-CNT-coated ASTM-SA213-T22 steel in a molten salt environment at 700° C," *International Journal of Minerals, Metallurgy, and Materials*, Vol. 26, No. 3, pp. 337-344, 2019.
- [4] M. DeCrescente and N. Bornstein, "Formation and reactivity thermodynamics of sodium sulfate with gas turbine alloys," *Corrosion*, Vol. 24, No. 5, pp. 127-133, 1968.
- [5] J. Cabral Miramontes, G. K. Pedraza Basulto, C. Gaona Tiburcio, P. D. C. Zambrano Robledo, C. A. Poblano Salas, and F. Almeraya Calderón, "Coatings characterization of Ni-based alloy applied by HVOF," *Aircraft Engineering and Aerospace Technology*, Vol. 90, No. 2, pp. 336-343, 2018.
- [6] K. Goyal, H. Singh, and R. Bhatia, "Current status of thermal spray coatings for high temperature corrosion resistance of boiler steel," *Journal of Material & Metallurgical Engineering*, Vol. 6, No. 1, pp. 29-35, 2016.
- [7] V. P. S. Sidhu, K. Goyal, and R. Goyal, "An investigation of corrosion resistance of HVOF coated ASME SA213 T91 boiler steel in an actual boiler environment," *Anti-Corrosion Methods and Materials*, Vol. 64, No. 5, pp. 499-507, 2017.
- [8] V. P. S. Sidhu, K. Goyal, and R. Goyal, "Comparative study of corrosion behavior of HVOF-coated boiler steel in actual boiler environment of a thermal power plant," *Journal of the Australian Ceramic Society*, Vol. 53, No. 2, pp. 925-932, 2017.
- [9] A. Nisar and K. Balani, "Phase and Microstructural Correlation of Spark Plasma Sintered HfB<sub>2</sub>-ZrB<sub>2</sub> Based Ultra-High Temperature Ceramic Composites," *Coatings*, Vol. 7, No. 8, p. 110, 2017.
- [10] Z. Yao, Y. Xu, Y. Liu, D. Wang, Z. Jiang, and F. Wang, "Structure and corrosion resistance of ZrO<sub>2</sub> ceramic coatings on AZ91D Mg alloys by plasma electrolytic oxidation," *Journal of Alloys and Compounds*, Vol. 509, No. 33, pp. 8469-8474, 2011.
- [11] J. Gao, Y. He, and D. Wang, "Fabrication and high temperature oxidation resistance of ZrO<sub>2</sub>/Al<sub>2</sub>O<sub>3</sub> micro-laminated coatings on stainless steel," *Materials Chemistry and Physics*, Vol. 123, No. 2-3, pp. 731-736, 2010.
- [12] C. Chang and S. Yen, "Characterization of electrolytic ZrO<sub>2</sub>/Al<sub>2</sub>O<sub>3</sub> double layer coatings on AISI 440C stainless steel," *Surface and Coatings Technology*, Vol. 182, No. 2-3, pp. 242-250, 2004.
- [13] N. Jeyakumar, A. C. Arumugam Kayambu, R. Ramasubbu, and B. Narayanasamy, "Thermal analysis of nanostructured alumina stabilized zirconia coating on exhaust manifold," *Energy Sources, Part A: Recovery, Utilization, and Environmental Effects*, Vol. 41, No. 7, pp. 854-865, 2019.
- [14] P. Niranatlumpong, C. Ponton, and H. Evans, "The failure of protective oxides on plasma-sprayed NiCrAlY overlay coatings," *Oxidation of Metals*, Vol. 53, No. 3-4, pp. 241-258, 2000.
- [15] W. Zhou, K. Zhou, C. Deng, K. Zeng, and Y. Li, "Hot corrosion behaviour of HVOF-sprayed Cr<sub>3</sub>C<sub>2</sub>-NiCrMoNb Al coating," *Surface and Coatings Technology*, Vol. 309, pp. 849-859, 2017.
- [16] V. P. S. Sidhu, K. Goyal, and R. Goyal, "Hot corrosion behaviour of HVOF-sprayed 93 (WC-Cr<sub>3</sub>C<sub>2</sub>)-7Ni and 83WC-17Co coatings on boiler tube steel in coal fired boiler," *Australian Journal of Mechanical Engineering*, pp. 1-6, 2017.